scientific reports

Check for updates

OPEN

In silico screening and molecular dynamics analysis of natural DHPS enzyme inhibitors targeting *Acinetobacter baumannii*

Saurabh Kumar Bhati[1], Farah Anjum[2], Anas Shamsi[3]✉, Md Imtaiyaz Hassan[4], Monika Jain[1], Jayaraman Muthukumaran[1], Rashmi Prabha Singh[5] & Amit Kumar Singh[1]✉

Over time, antimicrobial agents are losing their credibility in curbing infections due to the development of resistant pathogen strains. The resistant strains have proven to invade living beings and cause various diseases, leading to deaths at an alarming rate. *Acinetobacter baumannii* is one such pathogen, and to target it through enzyme inhibition, Dihydropteroate synthase enzyme's active site is virtually screened for antimicrobial agents against in-house libraries of natural molecules from medicinally important plants and *Agaricus spp.* fungus. Two ligands (MSID_000725 and CID_291096) are found to be suitable candidate inhibitors after various screening through Lipinski's based drug-like parameters, pharmacokinetic parameters, toxicity parameters and structural parameters which comprised of estimated free energy of binding, ligand efficiency and interaction analysis. DHPS enzyme catalyses the condensation reaction of hydroxymethyl-7, 8-dihydropterin pyrophosphate and para-aminobenzoic acid in the folic acid synthesis pathway in bacterial cells. The Complexes of the DHPS enzyme and ligands are validated through *in silico* studies, including MD simulations and MM/PBSA based binding free energy studies. The Complex DHPS-MSID_000725 and DHPS-CID_291096 were analysed for global dynamics attributes such as RMSD, RMSF, Rg, SASA and essential dynamics through PCA. The complexes were subjected to MM/PBSA based binding free energy analysis and were found to have binding free energy of -25.18 kcal/mol (DHPS-MSID_000725) and – 4.90 kcal/mol (DHPS-CID_291096).

Keywords MDR, *Acinetobacter baumannii*, DHPS enzyme, Virtual screening, MD simulation, MM/PBSA

Abbreviations

pABA	para-amino benzoic acid
DHPS	Dihydropterote synthase
ADME	Absorption, Distribution, Metabolism and Excretion
BBB	Blood Brain Barrier
GI	Gastro Intestinal
cLopP	Consensus octanol-water partition
TPSA	Topological polar surface area
CYP	Cytochrome enzymes

According to the Centre for Disease Control and Prevention (https://www.cdc.gov/hai/organisms/acinetobacter.html), *Acinetobacter* is a cosmopolitan bacterium with common habitats in soil and water. There have been many species of *Acinetobacter*, but mostly *A. baumannii* has substantially been the cause of diseases, accounting for the majority of infections in humans. It has been reported and found to be associated with infections of the

[1]Department of Biotechnology, Sharda School of Engineering and Technology, Sharda University, P.C. 201310, Greater Noida, U.P, India. [2]Department of Clinical Laboratory Sciences, College of Applied Medical Sciences, Taif University, P.O.Box 11099, Taif 21944, Saudi Arabia. [3]Centre of Medical and Bio-Allied Health Sciences Research, Ajman University, Ajman 364, United Arab Emirates. [4]Centre for Interdisciplinary Research in Basic Sciences, JamiaMilliaIslamia, Jamia Nagar, New Delhi 110025, India. [5]Department of Life Science, Sharda School of Basic Sciences and Research, Sharda University, P.C. 201310, Greater Noida, U.P, India. ✉email: anas.shamsi18@gmail.com; amitk.singh@sharda.ac.in

blood, urinary tract, lungs, and heart wall. This bacterium has been categorised into the list of pathogens which has been relevant in developing resistance to drugs used in its treatment. The susceptible people are the ones who are on breathing support machines, have devices such as catheters, have open wounds from surgery, are admitted to intensive and high-dependency units and have prolonged hospital stays. If environmental surfaces and shared equipment are not adequately cleaned, *A. baumannii* can persist for extended durations. Transmission of these germs from one individual to another can occur through contact with contaminated surfaces or equipment. Additionally, person-to-person spread is common, often facilitated by contaminated hands. Carbapenem-resistant *A.baumannii* was declared a critical prioritised pathogen in 2017 by the World Health Organisation, which stated that new antibiotics should be urgently developed[1]. Several antibiotics are being used to treat the infections caused by *A. baumannii*, such as colistin (commonly known as polymixin), which is effective in curbing *A. baumannii*, but the development of resistance against colistin has been reported[2]. *A. baumannii* is a gram-negative, aerobic, cocco-bacilli, non-motile. *A. baumannii* is a bacterium which respires aerobically, shows fastidious growth, gram-negative in nature concerning cell wall composition, and has cocco-bacilli shape[3]. It is one of the "ESKAPE" pathogens that show multiple and extensive drug resistance and are found to be associated with virulence factors[4].

Several key metabolic pathways essential for bacterial cell survival occur in the cytoplasm. One such biochemical pathway takes place in the cytosol to synthesise folic acid. Folic acid is one of the crucial components essential for the survival, growth and proliferation of bacterial cells. It is an important intermediate utilised in the synthesis of amino acids such as methionine, conversion of glycine to serine amino acid, double-ring nitrogenous bases, RNA and pantothenate. The final component of this metabolic pathway is Tetrahydrofolate (THF), which is used as a donor of carbon atoms during various metabolic conversions of substrates into products. Humans complete the dietary fulfilment of folic acid as they cannot synthesise folic acid due to the absence of a metabolic pathway[3]. The pathway is a multistep reaction, among which is an intermediate reaction involving condensation of pABA and HPPP to produce dihydropteroate. The reaction is catalysed by an enzyme known as Dihydropteroate Synthase (DHPS), which forms carbon-nitrogen bonds to carry out condensation reactions. The template DHPS enzyme from *Yersinia pestis* (Strain KIMD27) gives the structural features of the enzyme using the PDBsum server (http://www.ebi.ac.uk/thornton-srv/databases/pdbsum/)[5] and it consists of 2 sheets, six beta alpha beta units, one beta-hairpin, 10 strands, 12 helices, 20 helix-helix interacts, 22 beta turns. This enzyme has proven to be a suitable drug target for antibacterial agents like sulphonamides. Any inhibition effect on the enzymes involved in the metabolic production of folic acid would result in the lack of THF, thus affecting the survival mechanisms of bacterial cells. The DHPS enzyme is among the best characterised and proven drug targets for pathogens and bridges the link between the folic acid pathway and chorismate pathway; therefore, the failure of the bacteria to complete its life cycle could be caused by a unique inhibitory candidate targeting DHPS enzyme[6].

As per the statistics, it is extremely necessary to develop antibacterial agents against *A. baumannii*. Hence, in this study, we targeted the DHPS enzyme as a potential drug target. We conducted *in silico* studies on a three-dimensional predicted model of the DHPS enzyme by performing virtual screening against the DHPS binding site to find competitive inhibitors. The virtual screening was carried out against an *in-house* library consisting of natural ligand molecules. Natural compounds are often preferred over synthetic molecules as drug candidates because they tend to exhibit fewer side effects after consumption. Their complex structures and biological origins make them more compatible with human biochemistry, leading to better tolerance and reduced toxicity. Unlike synthetic molecules, which may cause adverse reactions, natural compounds are usually more selective in their interactions with biological targets. They play a significant role as ligand inhibitors in developing cures against pathogenic microbes and several other diseases by inhibiting the enzymes involved[7]. Most of the time, the synthetic compounds developed by pharmaceutical industries are very costly and become unaffordable for the majority of the population living below the poverty line[8]. These synthetic molecules also serve the problem of accessibility in various parts of the world as their production is localised to certain specific locations[9]. While there are existing studies on the DHPS enzyme from *Mycobacterium tuberculosis*, there remains a gap in exploring natural ligands targeting the DHPS enzyme in *Acinetobacter baumannii*. To address this, we screened and selected ligands, followed by molecular docking studies against the binding site of the DHPS enzyme in *A. baumannii*. The ligand-enzyme complexes were further validated through molecular dynamics (MD) simulations to assess structural stability and dynamics. Additionally, MM/PBSA-based binding free energy analysis was performed to evaluate binding affinities. This study, to the best of our knowledge, is the first to examine natural ligands for DHPS in *A. baumannii*, building on research from other organisms while exploring new therapeutic approaches for this pathogen[10].

Methodology

Structural prediction and identification of active site residues

The three-dimensional structure of the DHPS enzyme was downloaded from Alphafold (https://alphafold.ebi.ac.uk/entry/A0A0R4J6Y0), an *in silico* Protein Structure Database, by submitting the retrieved amino acid sequence from the Uniprot database (https://www.uniprot.org/uniprotkb/A0A0R4J6Y0/entry#sequences) by using the accession number A0A0R4JY60. The retrieved amino acid sequence was further used for finding homology to proteins from *Homo sapiens* using the Protein BLAST (BLASTp)[11]. The validation of the 3D model was performed using Structural Analysis and Verification sever (SAVES 6.0) (https://saves.mbi.ucla.edu/) and ProSA-Web server (https://prosa.services.came.sbg.ac.at/prosa.php)[12]. The SAVES 6.0 server contains various structure validation services, namely ERRAT[13], Verify 3D[14]and PROCHECK[15]. ProSA-Web server analyses protein structure by giving the Z score. The substrate binding groove of the enzyme was identified through a comprehensive literature review and pairwise sequence alignment with the template DHPS enzyme from *Yersinia pestis* (PDB ID:3tyz)[16]. To confirm the active-site residues, we performed multiple sequence alignment

S.No	Toxicity	Result
1.	Carcinogenicity	None
2.	Mutagenicity	None
3.	Reproductive effects	None
4.	Irritability	None

Table 1. Toxicological properties of the ligands used for virtual screening.

S.No	Parameter	Standard value
1.	GI	High
2.	BBB	Yes
3.	cLogP	Less than 5
4.	TPSA	Less than 100 $Å^2$
5.	CYP Inhibition	None
6.	ESOL	Soluble
7.	PAINS Alert	0

Table 2. Pharmacokinetic properties of the ligands that are put into the virtual screening.

of FASTA sequences from *A. baumannii*, *Yersinia pestis*, and *A. seifertii* to identify the conserved regions within the enzyme structure. Additionally, we overlaid the active-site residues of the 3D structure DHPS enzyme from *A. baumannii* with those from *Yersinia pestis* to further validate the conservation and structural alignment of the active site. The detailed results of this analysis have been presented in supplementary data.

Preparation of in-house library and grid box preparation for virtual screening

The molecules from the plants (phytochemicals) which showed an inhibitory effect on *A. baumannii* were identified through a literature review and downloaded from the IMPPAT server (https://cb.imsc.res.in/imppat/), and a molecular library containing natural ligands was prepared, and similar library of natural ligands from mushroom fungus (*Agaricus spp.*) with antibacterial properties was also prepared. The ligands in the constructed libraries demonstrated antibacterial activity against *A.baumannii*, which was confirmed through experimental validation. The literature review indicates that experimental validation typically involved Minimum Inhibitory Concentration (MIC) and Minimum Bactericidal Concentration (MBC) assays. Additionally, other analyses, such as microarray and immunohistochemical staining, were employed. Some ligands were further evaluated for their antibacterial properties through administration in mouse models suffering from conditions like urinary tract infections and renal inflammation[17–19]. The binding site of the DHPS enzyme was enclosed in the Grid box, prepared with the help of PyRx software[20]to screen for the ligands which could bind to the defined location enclosed within the Grid box. The centre and size dimension coordinates were determined to encompass the active site groove. This grid box, which was designed around the active site, was used to screen the ligands out of libraries that were capable of binding to the targeted site. The centre coordinates for the x, y and z axis were 14.93 (Å), 9.00 (Å), and 42.45 (Å), respectively. The size dimensions for the x, y and z axis were 28.63 (Å), 21.41 (Å), and 25.00 (Å), respectively.

Virtual screening and pharmacokinetics

The in-house library consists of natural molecules, which were first put through screening of the ligands to find out which ligands possessed drug-like properties. The ligand molecules in the library were screened using the Data Warrior tool (https://openmolecules.org/datawarrior/)[21]based on Lipinski's rule of five[22] as well as toxicological properties (carcinogenicity, mutagenicity, reproduction ability, irritability). The libraries were further screened for ligands with ADME (Absorption, Distribution, Metabolism and Excretion) characteristics by employing the SwissADME server (https://www.swissadme.ch/)[23]. The ligands were also scrutinised through other parameters like BBB (Blood Brain Barrier) permeability, Gastro-Intestinal (GI) absorption, solubility in hydrophilic vicinity, cLopP (Consensus octanol-water partition coefficient) value, topological polar surface area (TPSA), CYP enzymes inhibition and PAINS alert. The parameters used to assess toxicity are presented in Table 1, while Table 2 illustrates the pharmacokinetic properties of the ligands. The selected ligands were further screened against the defined grid box with specific coordinates enclosing the active site of the DHPS enzyme to search for ligands which could bind to the enzyme, compete with substrate molecule and inhibit its catalytic activity.

Molecular Docking of the ligand with the active site of the DHPS enzyme

The selected ligands were docked using MGLTools 1.5.7 and AutoDock 4.2.6[24], and the docking search was restricted to the active site of the DHPS enzyme. The grid box with well-defined centre and size dimension coordinates was constructed to enclose the active site of the DHPS enzyme. The docking was governed according to the Lamarckian Genetic Algorithm (LGA), configured to 1000 runs with a population size of 200. The maximum number of 27,000 generations was kept, and the maximum number of energy evaluations was kept to

2,500,000. The rate of gene mutation and crossover was fixed at 0.2 and 0.8, respectively. The analysis of docked complexes was done using MGLTools 1.5.7 and further selected ligands were put forward for interaction studies.

Interaction studies between DHPS enzyme and ligands

The complexes formed between the DHPS enzyme and the selected ligands were subjected to detailed interaction studies. These studies illustrate the interactions between ligand atoms and the active site residues of the DHPS enzyme. The interactions examined include hydrogen bonds, which are crucial for stabilizing the complex, as well as van der Waals interactions. Although van der Waals forces are not as strong as hydrogen bonds, they play a significant role in stabilizing the protein-ligand complexes. Additionally, π-π and alkyl interactions were also assessed, as they contribute to the overall stability of the complexes.

Prioritization of ligand molecules for further validation studies

Following the AutoDock and interaction studies, two ligands were shortlisted for subsequent molecular dynamics (MD) simulation studies. The estimated binding free energy obtained from AutoDock served as a primary criterion for the final selection of these ligands. The interaction studies provided insights into the bonds formed between the DHPS enzyme and the ligands, highlighting the stabilization of the complexes based on bond orientation and the number of interactions. Ultimately, these two ligands in complex with the DHPS enzyme were selected for further simulation studies to evaluate their dynamic behavior and stability.

MD simulation

The selected ligands were put in a complex with the active site of the DHPS enzyme, and these complexes, along with the unbound DHPS enzyme, were subjected to 100ns molecular dynamics simulation by employing GROMACS 2021.3[25]. MD simulation demonstrates the behaviour of proteins and their complexes with ligands in virtual physiological conditions. The topology of the ligand molecules was obtained utilising the SwissParam server (https://www.swissparam.ch/)[26]. The parameterisation of the DHPS enzyme was done using the CHARMM27 force field. CHARMM27 offers meticulously calibrated force fields that are highly detailed, covering various bimolecular systems such as proteins, nucleic acids, lipids, and carbohydrates. This comprehensive parameterisation guarantees precise simulation of a wide array of molecular interactions and structural conformations. The accuracy of the CHARMM27 force field has been thoroughly confirmed through comparisons with experimental data, including X-ray crystallography, NMR spectroscopy, and thermodynamic measurements. This validation guarantees that simulations offer accurate and dependable insights into the behaviour of proteins[27]. DHPS enzyme was enclosed within a cubic cell with a –d value of 1.0 for simulation. The protein system was solvated next, and the TIP4P water model was employed for this. TIP4P is a rigid 4-site transferable intermolecular model with virtual conditions of water model at standardised pressure. Out of the 4 points, one point is for the oxygen atom, and three are other charge sites, and it maintains equal charge distribution throughout the system. This water model embodies one dummy atom and three water molecules to mimic the actual water conditions. This model virtually demonstrates the solvation and density at 298 K and one atmospheric pressure, and it is a balance of computational expense and reliability[28]. Then, the protein was neutralised to achieve a net charge of zero using the gmx genion command of GROMACS. First, the net charge of the system was determined, and then the *genion* module replaced solvent molecules with appropriate counterions to neutralise the charge. A maximum of 50,000 iterations of the steepest descent-based minimization technique were used to lower the energy of DHPS and DHPS enzyme-ligand complexes to reach a tolerance threshold of 100 kJ/mol[29]. This approach to lowering the energy is enough to take enzymes into minimal energy, attaining an optimised state. This also removes the stearic clashes and hindrances within the chains of the enzymes. Together with a decrease in constraints, the steepest descent algorithm can lower the energy levels of proteins and enzyme-ligand complexes, allowing them to move from an extremely distorted and energetically unfavourable state to a more stable, minimal-energy state under a variety of circumstances. Next, the system was put into equilibration for 1ns with 50,000 set steps, done through two steps. First, equilibration was done at constant volume and temperature (NVT) and second at constant pressure and temperature (NPT). Then, 100 ns production MD simulations were run using two femtosecond time increments, and the trajectories that emerged were taken into consideration for additional research and were analysed through various built-in functions of GROMACS 2021.3[29]. Various global and essential dynamics parameters were analyzed to predict the physiological behaviour of the DHPS enzyme and its complexes with ligand molecules during 100 ns simulations. Key parameters assessed included Root Mean Square Deviation (RMSD), Root Mean Square Fluctuation (RMSF), Radius of Gyration (Rg), Solvent Accessible Surface Area (SASA), hydrogen bonds, and essential dynamics. The results were visualized as 2D graphs using QtGrace.

MM/PBSA approach to calculate the binding free energy of the complexes

The *g_mmpbsa* tool[30]evaluated the binding free energy of DHPS enzyme complexes during their interaction. This tool uses the MM/PBSA (Molecular mechanics / Poisson-Boltzmann surface area) approach to compute the binding free energy during MD simulation. The g_mmpbsa module can also be utilized to perform reside energy decomposition analysis[31].

The calculations were done using the following equation:

$$\Delta\, \mathrm{G}_{binding} = \Delta\, E_{ele} + \Delta\, E_{vdw} + \Delta\, G_{pol} + \Delta\, \mathrm{G}_{np} \quad (1)$$

In the equation above, $\Delta G_{binding}$ denotes the binding free energy of DHFR complexes, while $\Delta E_{ele,}$ $\Delta G_{pol,}$ $\Delta G_{np,}$ ΔE_{vdw} stands for changing electrostatic energy, polar solvation energy, non-polar solvation energy, and van der Waals energy, respectively. The dielectric constants for the solvent and solute, employed for calculating different

energy transition factors, were 80 and 2, respectively. To estimate the binding free energy using the MM/PBSA method, 1000 frames from the converged MD trajectories, specifically from 80 ns to 100 ns, were selected at intervals of 50 ps. To further validate the positioning of the prioritized candidates in the active site of the drug target protein, we performed a time-frame analysis using regular intervals. Moreover, this analysis was used to monitor whether the ligands remained close to and stayed within the active site throughout the MD simulation. Structural snapshots were retrieved at various intervals, including 0 ns, 25 ns, 50 ns, 75 ns, and 100 ns, to confirm the stability of the ligands in the active site and their sustained interactions with the enzyme.

Results and discussion

Structure prediction and active site analysis

The three-dimensional DHPS enzyme was found non-homologous to proteins in *Homo sapiens*. The Enzyme model, when analysed through the SAVES 6.0 server, resulted in an ERRAT score of 99.62, a Verify 3D score of 91.87%, and Procheck results including errors, warning and pass as 0, 3, and 5 respectively. According to the Ramachandran plot, 94% of residues were in favoured regions, 6% were in additional allowed regions, and no residues were found in generously allowed and disallowed regions. The ProSA web server resulted in a Z score of −9.42 and revealed the model quality of protein as good. The active site residues are Phe36, Pro72, Lys228, Phe195 and Ser226, which were identified using a literature review and sequence alignment. The three-dimensional structure of the enzyme along with active site residues is given in the supplementary data (Sect. 2). The sequence alignment results between the target with the template enzyme from *Yersinia pestis* (PDB ID: 3TYZ) are provided in the supplementary data (Sect. 1(i)). The sequence alignment of *A. baumannii* with *Yersinia pestis* and *A. seifertii*, obtained using the Multalign along with ESPRIPT tool, is also detailed in the supplementary data (Sect. 4). Additionally, the results of the overlaid active-site residues for the three-dimensional structure of DHPS enzyme from *A. baumannii* and *Yersinia pestis* are presented in supplementary data (Sect. 1(ii)). The three-dimensional structure and electrostatic surface potential map of the DHPS enzyme are shown in Fig. 1 below.

Virtual screening and pharmacokinetics

Only those ligands in the libraries that successfully passed the Data Warrior tool screening, based on Lipinski's rule of five and various parameters from the SwissADME server (including absorption, distribution, metabolism, and excretion), were considered for evaluation against the active site of the DHPS enzyme. Additional criteria included blood-brain barrier (BBB) permeability, gastrointestinal (GI) absorption, solubility in hydrophilic environments, consensus octanol-water partition coefficient (cLogP) value, topological polar surface area (TPSA), inhibition of CYP enzymes, and PAINS alerts. After applying these filters, we identified 16 molecules that exhibited strong binding affinity to the enzyme's active site. The binding energies of the interactions between

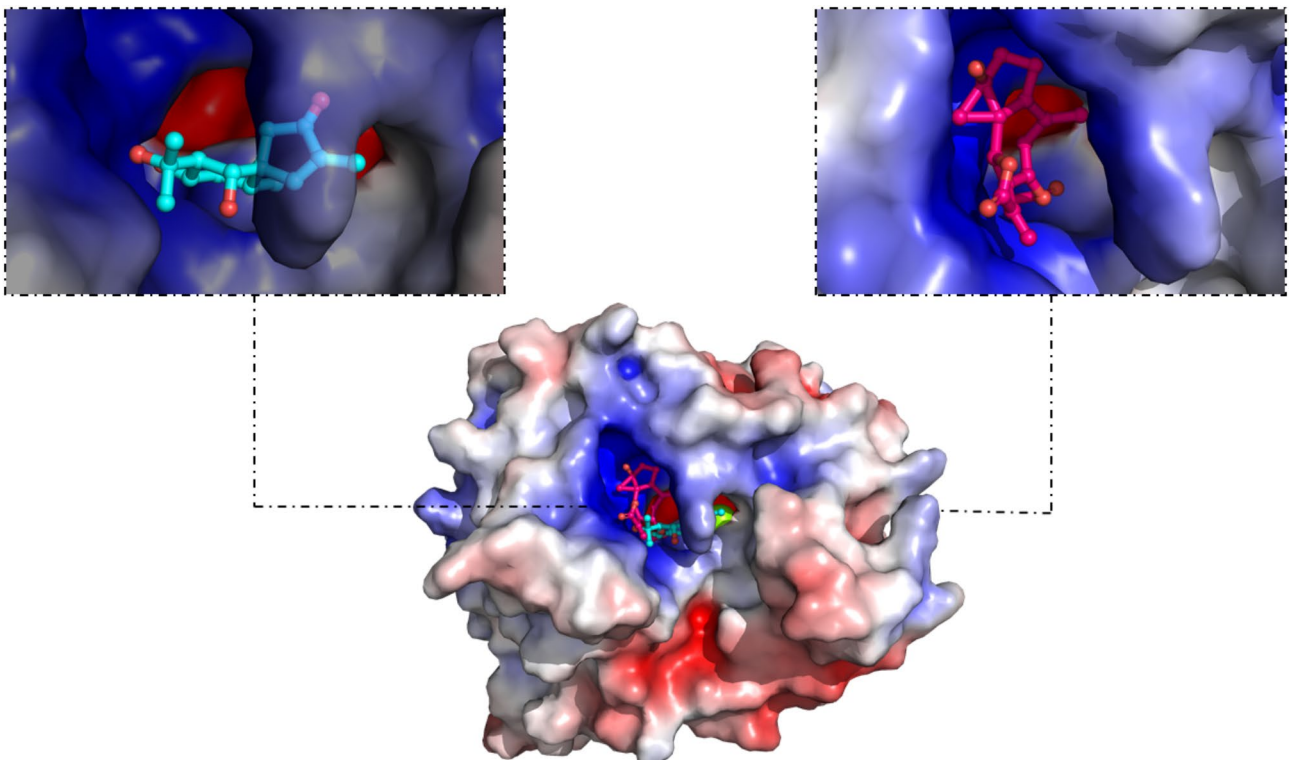

Fig. 1. Electrostatic surface potential map of the DHPS enzyme illustrating the binding of ligands at the active site. The ligand MSID_000725 is represented in cyan, while CID_291096 is shown in pink.

S.no	Ligand	Estimated Binding energy (AutoDockVina) (kcal/mol)	Estimated binding energy (AutoDock) (kcal/mol)	Ki (μM)	Ligand efficiency parameter
1	CID_291096	−7.3	−7.42	3.87	0.34
2	MSID_000725	−6.8	−7.06	24.09	0.37
3	MSID_000733	−6.9	−6.04	60.83	0.32
4	MSID_000738	−6.8	−6.26	35.52	0.31

Table 3. Molecular Docking results of selected ligands and their binding affinity values obtained from both AutoDock and AutoDockVina programs.

S.no	Ligands	Hydrogen bonds	Distance (Å)	Pi-Pi alky interactions	Distance (Å)	Van der waal interactions
1	CID_291096	Arg243 Gly196 Arg263	3.13 2.97 2.98	Lys228 Phe197 Arg71	3.46, 5.48 4.54 4.40	Arg229 Met155 Pro72 Thr70 Ile28 Ser226 His265 Ala240 Arg227
2	MSID_000725	His265 Thr70 Ser226	2.13 3.32 1.95, 1.92	Arg227 Ile28 Arg71 His265	3.91 5.32, 4.19 4.68 4.16, 4.58	Ser69 MGA279 Lys228 Asn30 Arg263
3	MSID_000733	Arg263 Ser226 Lys228	5.83 2.16, 1.85 2.68	Arg71 Arg227 His265 Phe197 Lys228	5.06 4.11 4.48 4.78 4.98	Ser69 Ala240 Arg243 Met155 Ile28 Thr70
4	MSID_000738	Gly196 Ser226 Arg263	2.13 2.12 2.82	Arg71	4.70	Arg229 Arg227 Lys228 His265 Ile28 Asn30 Thr70 Phe197 Pro72 Met155

Table 4. Selected ligands with their bonding interactions with DHPS enzyme mentioned along with distance in Angstrom (**Å**).

the ligands and the DHPS enzyme, as determined during virtual screening, ranged from −4.4 kcal/mol to −7.3 kcal/mol.

Molecular Docking of the ligand with the active site of the DHPS enzyme

From the initial pool of 16 molecules, we selected four ligands with the most favourable negative binding energies for AutoDock-based molecular docking studies. The chosen ligands included CID_291096 (−7.3 kcal/mol), MSID_000733 (−6.9 kcal/mol), and MSID_000725 and MSID_000738, both exhibiting a binding energy of −6.8 kcal/mol. Detailed information regarding these ligands is presented in Table 3. In a related study, the DHPS enzyme from *Mycobacterium leprae* was analyzed using AutoDock alongside the FDA-approved drug Clofazimine, which demonstrated a binding affinity of −9.0 kcal/mol[10]. Therefore, the DHPS-CID_291096 and DHPS-MSID_000725 complexes exhibit commendable binding affinities, as supported by the AutoDock results represented in Table 3.

Study of interaction between DHPS enzyme and ligands

The interaction analysis of the DHPS enzyme in complex with the ligands CID_291096, MSID_000725, MSID_000733, and MSID_000738 identified the types of bonds formed during these interactions, including hydrogen bonds, van der Waals interactions, and π-π alkyl interactions. Details regarding the specific bonds established between the DHPS enzyme and each ligand are provided in Table 4 below.

Selection of the final ligand molecules for validation studies

Following the molecular docking and interaction analyses, the two most promising ligands were selected for further molecular dynamics (MD) simulation studies. The ligands CID_291096 and MSID_000725 exhibited the highest binding affinities of −7.42 kcal/mol and −7.06 kcal/mol, respectively, among the four candidates. CID_291096 demonstrates stable interactions characterized by the formation of hydrogen bonds with the residues Arg243, Gly196, and Arg263, with bonds oriented from three distinct directions. This stable state is

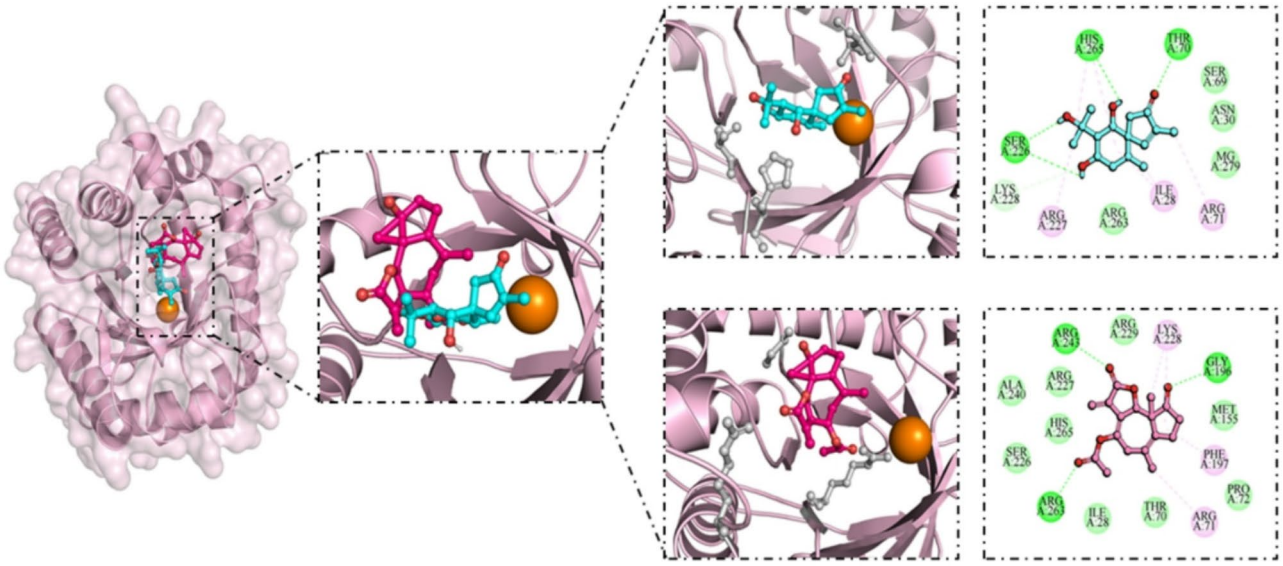

Fig. 2. Structural representation of the DHPS enzyme, highlighting the magnesium ion (Mg^{2+}) as a cofactor in orange. The ligands are depicted in the binding pocket, with ligand MSID_000725 shown in cyan and ligand CID_291096 in pink. The figure illustrates the bonds formed during interactions between the ligands and the enzyme, showcasing the crucial interactions that contribute to the stability of the ligand-enzyme complexes.

S.no	Ligand	Molecular weight	Molecular formula
1	MSID_000725	268.35 g/mol	$C_{15}H_{24}O_4$
2	CID_291096	306.4 g/mol	$C_{17}H_{22}O_5$

Table 5. Ligand's molecular weight and molecular formula.

further enhanced by π-π alkyl interactions with residues Lys228, Phe197, and Arg71, as well as van der Waals interactions with Arg229, Met155, Pro72, Thr70, Ile28, Ser226, His265, Ala240, and Arg227.

Similarly, the ligand MSID_000725 achieves stable interactions through hydrogen bonds with Ser226, His65, and Thr70, originating from four different directions within the active binding site. Notably, Ser226 contributes two hydrogen bonds. Additionally, the interaction is supported by π-π alkyl interactions with Arg227, Ile28, Arg71, and His265, along with van der Waals interactions involving Ser69, MGA279, Lys228, Asn30, and Arg263 (where MG refers to the magnesium ion, a cofactor of the enzyme). The interactions between the protein and ligand complexes are illustrated in Fig. 2 below.

Both ligands demonstrate permeability across the blood-brain barrier (BBB), exhibit gastrointestinal (GI) absorption, and show solubility in a hydrophilic environment. Additionally, they possess a consensus octanol-water partition coefficient (cLogP) value of less than 5, a topological polar surface area (TPSA) under 100 Å, do not inhibit CYP enzymes, and do not trigger any PAINS alerts. Details regarding the selected ligands are provided in Table 5.

Molecular dynamics simulation

The study employed molecular dynamics simulations to investigate the atomic changes in whole macromolecules over a defined period under physiological conditions. This approach allows for the evaluation of the strength, stability, and interaction patterns of protein-ligand complexes. It also facilitates the elucidation of conformational changes that macromolecules undergo in a hydrophilic biological environment. Various structural properties were analysed including global dynamics attributes such as root mean square deviation (RMSD), root mean square fluctuation (RMSF), radius of gyration (Rg), and solvent-accessible surface area (SASA), alongside essential dynamics characteristics such as principal component analysis (PCA).

Root mean square deviation

RMSD is the deviation of atoms in the protein structure from their positions when subjected to MD simulation in both unbound and bound states. The unbound DHPS enzyme shows a mean RMSD of 0.18 nm and a stable trajectory with slight fluctuations; however, there is an overall increase in the deviation from the start to the end of the simulation. The DHPS enzyme and ligand MSID_000725 complex show an unstable trajectory, suggesting significant structural changes in the protein due to ligand interaction. From 17 ns to 55 ns, the trajectory is stable, but after that, it exhibits a sudden spike around 65 ns and then returns to the previous axis. The mean RMSD for this complex is 0.23 nm, which is higher than that of the unbound enzyme. The DHPS enzyme and

ligand CID_291096 complex show a mean RMSD of 0.26 nm, which is the highest among the three comparisons; however, compared to the DHPS-MSID_000725 complex, the trajectory depicts a stable pattern. Until 35 ns, the RMSD value increases up to 0.28 nm, but then it decreases until 55 ns and attains stability until the end of the simulation. In a comparative reference study, the DHPS-Clofazimine complex from *Mycobacterium leprae* shows a mean RMSD of 0.54 nm. In comparison, our RMSD values are much lower than one for the FDA-approved drug Clofazimine against the DHPS of *Mycobacterium leprae*. The DHPS enzyme in an unbound state shows a lower RMSD, which increases after interaction with the ligands, indicating that the enzyme undergoes conformational changes in structural parameters, with both ligands inducing a similar amount of dynamics. The trajectories are shown in Fig. 3a. Thus, it is clear that both ligands are interacting with the enzyme to achieve stability.

Root mean square fluctuation

In molecular dynamics simulations, the average deviation of atomic positions from their mean positions over time is measured by a metric called root mean square fluctuation (RMSF). This parameter provides insights into the dynamics and flexibility of a protein structure, making it crucial for assessing the stability of proteins in both native and bound states. The unbound DHPS enzyme shows a mean RMSF of 0.12 nm, but some residues, such as Asp38 (0.30 nm), Arg229 (0.33 nm), Gln283 (0.51 nm), Thr70 (0.29 nm), and Pro72 (0.29 nm), exhibit significant fluctuations. The complex of the DHPS enzyme and ligand MSID_000725 has a mean RMSF of 0.12 nm, which is similar to that of the native DHPS enzyme. During the interaction, the residues that show significant fluctuations include Thr70 (0.32 nm), Gln236 (0.37 nm), and Pro239 (0.38 nm). The complex of the DHPS enzyme and ligand CID_291096 shows a mean RMSF of 0.11 nm, which is the lowest among all comparisons, suggesting a stable interaction between the enzyme and the ligand. Residues such as Gln15 (0.28 nm), Arg229 (0.30 nm), and Gln283 (0.37 nm) exhibit noticeable oscillations. All the residues mentioned above, which show prominent fluctuations, are located in the secondary loop regions, which are flexible by nature. The trajectories of the

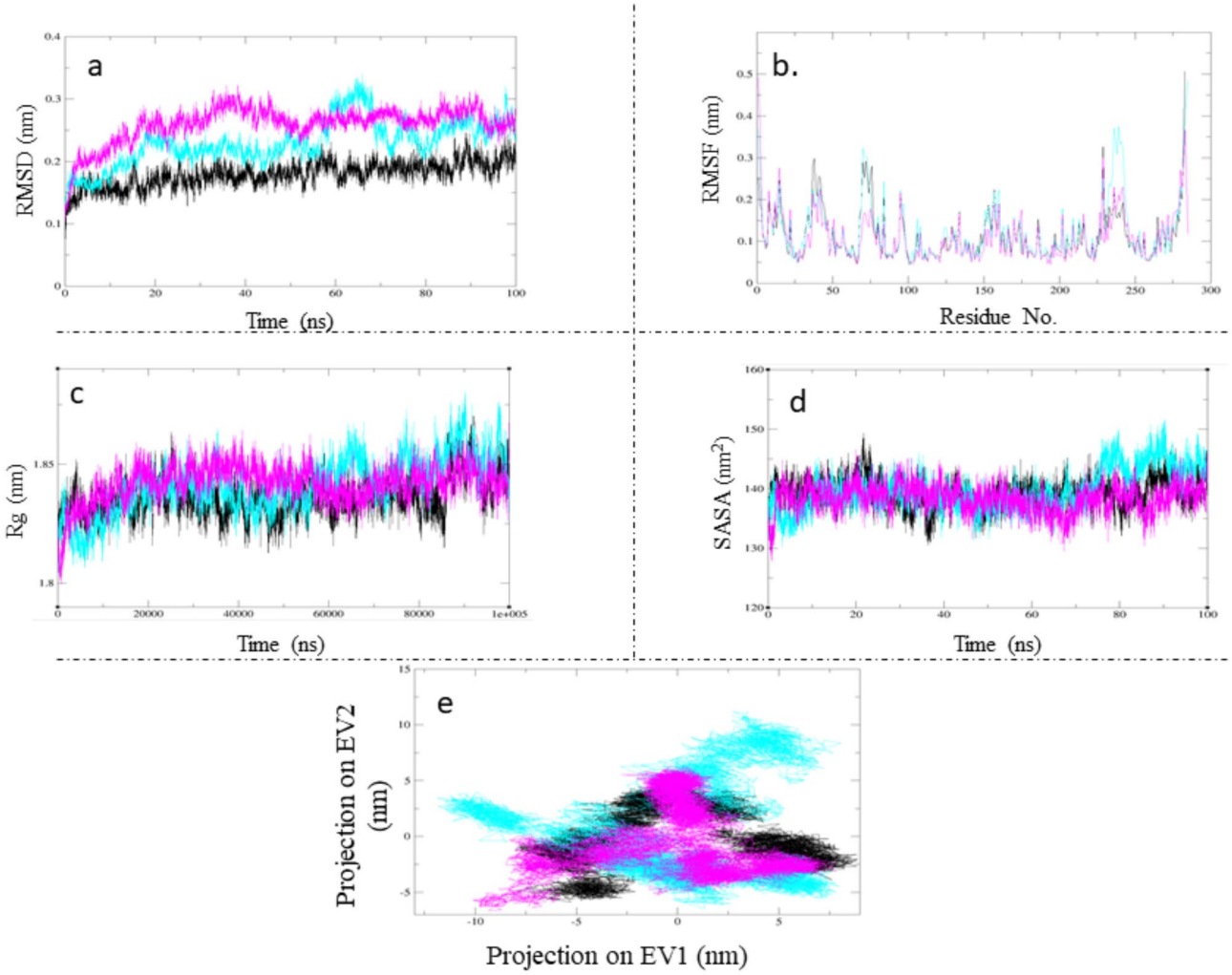

Fig. 3. MD simulation analysis of the DHPS enzyme with different ligands: (a) RMSD, (b) RMSF, (c) Rg, (d) SASA, (e) PCA. Color code: Unbound DHPS (Black), Ligand MSID_000725 (Cyan), Ligand CID_291096 (Pink).

fluctuations are shown in Fig. 3b. The average fluctuation exhibited by the unbound and bound DHPS enzyme suggests that they have a stable encounter, inducing variations in the secondary loop regions, while the stable region residues undergo normal deviations. In a reference study, the DHPS-Clofazimine complex shows a mean RMSF of 0.14 nm, which is slightly higher than the ligands in our study[10].

Radius of gyration

The radius of gyration (Rg), measured for the protein backbone, indicates how compact the protein structure is. Therefore, assessing the compactness of the protein conformation during simulations in both unbound and bound states is crucial for determining the nature of ligand interactions with the protein's active site, as well as its behavior in a physiological environment. An increase in Rg signifies greater conformational changes, while a decrease indicates less conformational dynamics in the protein's structural parameters. The DHPS enzyme in its unbound state has a mean Rg value of 1.84 nm, and the trajectory obtained shows a stable pattern, except for a slight spike observed between 85 ns and 95 ns. In contrast, the complex of DHPS with the ligand MSID_000725 shows a mean Rg of 1.84 nm but exhibits unstable deviations, both upward and downward, making it less stable than the native DHPS enzyme. The complex of the DHPS enzyme with ligand CID_291096 also has a mean Rg of 1.84 nm; however, its trajectory pattern demonstrates much greater stability compared to the DHPS-MSIC_000725 complex. Thus, the analysis of the radius of gyration suggests that the DHPS enzyme experiences residual fluctuations upon interacting with the ligands. Despite these fluctuations, both the unbound and bound states exhibit similar mean values, indicating stable interactions between the enzyme and the ligands. In a reference study of the DHPS-Clofazimine complex, the mean Rg value was found to be 1.75 nm, which is slightly lower but comparable to our ligands and the unbound enzyme[9]. The trajectory pattern for the Rg parameter is depicted in Fig. 3c.

Solvent accessible surface area

SASA illustrates the variation in enzyme structure concerning conformational changes caused by ligand binding and solvent interactions between the DHPS enzyme and DHPS-ligand complexes. The unbound DHPS enzyme under virtual physiological conditions shows a mean SASA profile of 139.21 nm^2. The SASA pattern remains stable, except for a spike at 20 ns and a drop at 37 ns. The complex of the DHPS enzyme with ligand MSID_000725 exhibits a mean SASA profile of 139.80 nm^2. The trajectory of this complex is unstable compared to the unbound DHPS enzyme; for the first 75 ns, the pattern is almost stable with minor fluctuations, while the last 25 ns show occasional surges and drops. In contrast, the complex of the DHPS enzyme with ligand CID_291096 shows an average SASA profile of 138.22 nm^2, which is slightly lower than that of the DHPS-MSID_000725 complex and comparable to the unbound DHPS enzyme. This suggests a stable interaction between the ligands and the protein, resulting in less conformational dynamics when interacting with the physiological environment's solvation. Additionally, the SASA profile of the DHPS-Clofazimine complex shows a mean value of 121.57 nm^2, which is slightly lower than that of both the unbound DHPS and the bound DHPS enzyme[9]. The SASA profile pattern is shown in Fig. 3d.

Principal component analysis

Since an enzyme's functioning mainly results from the collective atomic movements it experiences, motion analysis is typically used to assess the stability of enzyme and ligand complexes represented from high dimensional subspace to low dimensional subspace. The native DHPS enzyme's C-alpha atoms move, and this movement is used in the PCA approach to depict changes. The PCA analysis matrix represents two eigenvectors (PC1 and PC2) with corresponding eigenvalues that are utilized to investigate the important motions relevant to the DHPS enzyme system. The native DHPS enzyme and the enzyme-ligand complexes (DHPS-MSID000725 and DHPS-CID_291096) are found to have traces of diagonalised covariance matrices as 94.19 nm^2, 118.96 nm^2 and 91.24 nm^2, respectively. Figure 3e displays the distribution of changes in the covariance matrix for free DHPS enzyme and DHPS enzyme-ligand complexes. The PCA analysis suggest that the DHPS-CID_291096 shows the least eigenvalues of PC1 and PC2 eigenvectors, even less than the unbound DHPS enzyme, while the complex DHPS-MSID000725 has the maximum eigenvalues. From this, it can be seen that ligand CID_291096 induces less structural dynamics after interaction with the DHPS enzymes. The ligand MSID_000725 seems to induce a bit of high variation in the structural dynamics of the DHPS enzyme. Through PCA analysis, it was evident that both ligands induced stability after interaction with the enzyme.

MM/PBSA approach to calculate the binding free energy of the complexes

The *g_mmpbsa* tool, which was utilised for calculating binding energy, gave the summarised binding energy for DHPS-MSID000725 and DHPS-CID_291096 as −25.19 kcal/mol and − 4.90 kcal/mol, respectively. The amino acid residue decomposition analysis is provided in the supplementary data (Sect. 3). The results indicate that the functionally important residues of the drug target protein play a major role in binding with the lead candidates. The various contributing energies in kcal/mol are given in Table 6 below.

The binding energy indicates that both ligands interact with negative free binding energy to the target protein. For the ligand MSID_000725, the maximum energy contribution comes from electrostatic energy, while for the ligand CID_291096, the majority of the contribution is from Van der Waals energy. The ligand MSID_000725 binds with a higher negative binding energy compared to ligand CID_291096, signifying a stable binding and spontaneous encounter with the active binding groove of the DHPS enzyme. The trajectory of the various binding energies for both ligands is shown in Fig. 4. The binding energy from AutoDock analysis for the DHPS-Clofazimine complex was found to be −9.0 kcal/mol[9]. Considering this, it is evident that ligand MSID_000725 demonstrates a much more stable interaction due to its high negative binding energy, while ligand CID_291096 exhibits slightly less negative binding energy than the DHPS-Clofazimine complex but still

S.no	Complex	Van der Waal energy	Electrostatic energy	Polar Solvation energy	SASA energy	Binding energy
1	DHPS-MSID_000725	−1.63 +/- 3.73	−80.21 +/- 7.31	57.98 +/- 5.54	−1.33 +/- 0.41	−25.18 +/- 4.88
2	DHPS-CID_291096	−22.02 +/- 2.30	−5.40 +/- 3.36	25.86 +/- 14.76	−3.35 +/- 0.29	−4.90 +/- 14.11

Table 6. MM/PBSA contributing energies during binding of DHPS enzyme and ligand (Energies are mentioned in kcal/mol).

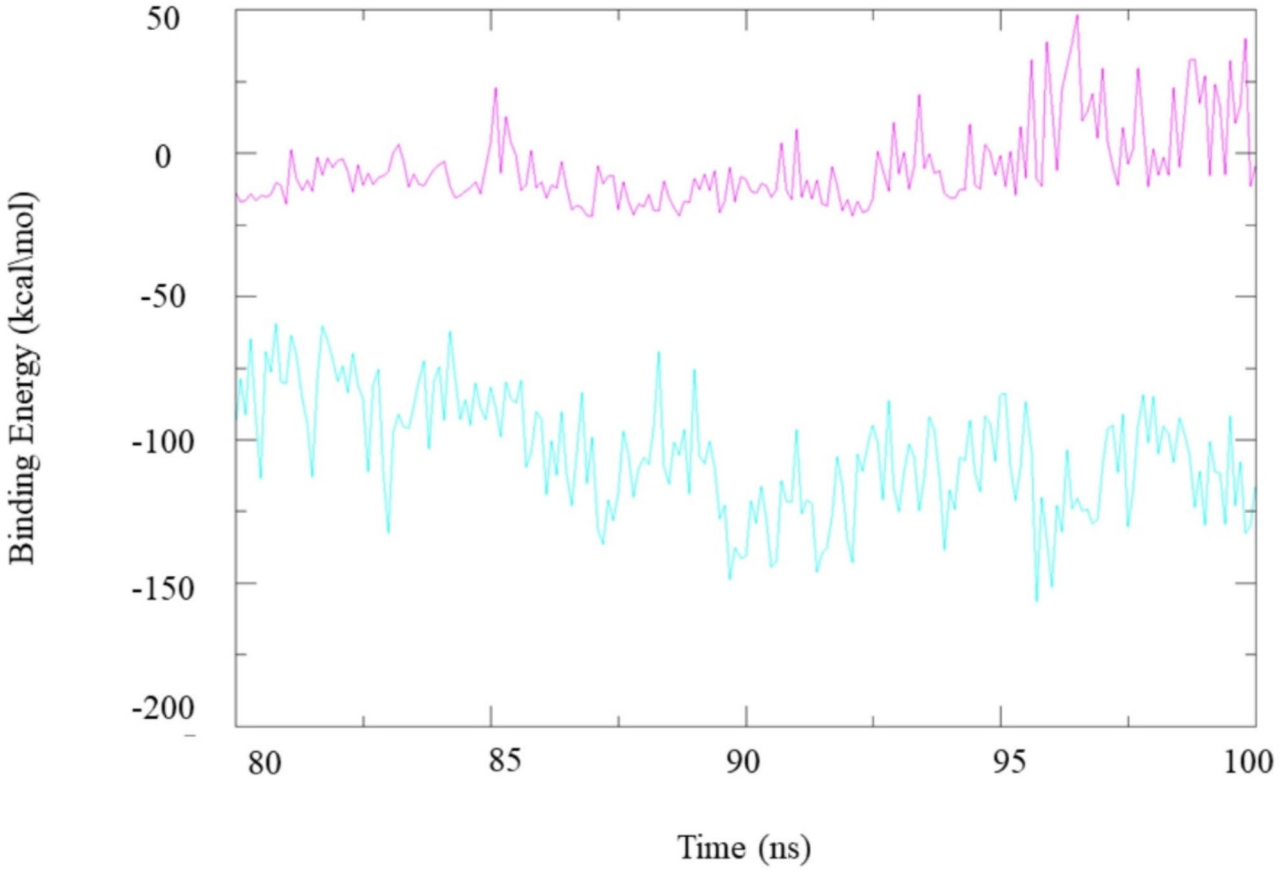

Fig. 4. Binding Energy Analysis Using MM/PBSA:.

interacts spontaneously. The snapshot's time-frame analysis has been included in supplementary data (Sect. 5) (Table 1). The results of the time-frame analysis demonstrated that the prioritized lead candidate binds strongly to the drug target protein and is properly oriented within the binding pocket.

Color Legend: DHPS-MSID_000725 is represented in Cyan, and DHPS-CID291096 is represented in Pink.

Conclusion

The increasing trend of antimicrobial resistance has created an urgent need to develop novel antimicrobial agents. In our present study, we targeted *A. baumannii*, which has been declared a serious health hazard by various health agencies. In this study, the DHPS enzyme, an essential biocatalyst in the survival mechanisms of bacteria, is targeted, modelled, and virtually screened against constructed libraries of ligands. The resultant ligands were screened based on pharmacokinetics and were shortlisted further through molecular docking analysis using AutoDock and interaction analysis. Ultimately, two ligands, MSID_000725 and CID_291096, were selected. The DHPS-CID_291096 and DHPS-MSID_000725 complexes possessed binding affinities of −7.42 kcal/mol and −7.06 kcal/mol, respectively. Both ligands, upon interaction with the DHPS enzyme, showed reliable interaction through bond formation. The MD simulation parameters, such as RMSD, RMSF, Rg, SASA, and PCA, evaluated both ligands as potential drug candidates. The study was also compared to a counter study on the DHPS enzyme from *Mycobacterium leprae* in complex with the FDA-approved drug Clofazimine, and the comparisons suggested somewhat similar outcomes, thus strengthening the results of our study. Through MM/PBSA based binding free analysis, it was found that the complex DHPS-MSID_000725 has a binding energy of −25.18 kcal/mol, while DHPS-CID_291096 had a binding affinity of −4.90 kcal/mol, indicating that both ligands are binding spontaneously with the active site of the enzyme. Thus, it can be concluded that MSID_000725 and CID_291096

can both be considered potential drug candidates, with MSID_000725 binding more spontaneously. This study was conducted under *in silico* conditions, relying on a predicted DHPS enzyme. However, these conditions have inherent limitations in fully replicating actual physiological environments. Therefore, further experimental studies and pre- and clinical trials are necessary to validate the in silico-driven hypothesis. Additionally, natural molecules identified as promising drug candidates in preliminary studies should undergo extensive validation before being considered for further development as viable drug molecule[32].

Data availability

The corresponding author will provide data whenever it is required.

Received: 29 October 2024; Accepted: 17 February 2025
Published online: 05 March 2025

References

1. Ma, C. & McClean, S. Mapping global prevalence of acinetobacterbaumannii and recent vaccine development to tackle it. *Vaccines* **9** (6), 570 (2021).
2. Jiang, Y. et al. Carbapenem-resistant acinetobacterbaumannii: A challenge in the intensive care unit. *Front. Microbiol.* **13**, 1045206 (2022).
3. Bhati, S. K., Jain, M., Muthukumaran, J. & Singh, A. K. A computational perspective towards the identification of promising lead molecules against 6-hydroxy-methyl Dihydropterinpyrophosphokinase (HPPK) from acinetobacterbaumannii. *J. Biomol. Struct. Dynamics*. **21**, 1–0 (2023 Jul).
4. Ibrahim, S., Al-Saryi, N., Al-Kadmy, I. M. & Aziz, S. N. Multidrug-resistant acinetobacterbaumannii as an emerging concern in hospitals. *Mol. Biol. Rep.* **48** (10), 6987–6998 (2021).
5. Laskowski, R. A., Jabłońska, J., Pravda, L., Vařeková, R. S. & Thornton, J. M. PDBsum: structural summaries of PDB entries. *Protein Sci.* **27** (1), 129–134 (2018).
6. Bertacine Dias, M. V., Santos, J. C., Libreros-Zuniga, G. A., Ribeiro, J. A. & Chavez-Pacheco, S. M. Folate biosynthesis pathway: mechanisms and insights into drug design for infectious diseases. *Future Med. Chem.* **10** (8), 935–959 (2018).
7. Baier, A. & Szyszka, R. Compounds from natural sources as protein kinase inhibitors. *Biomolecules* **10** (11), 1546 (2020).
8. Karimi, A., Majlesi, M. & Rafieian-Kopaei, M. Herbal versus synthetic drugs; beliefs and facts. *J. Nephropharmacology*. **4** (1), 27 (2015).
9. Thompson, H. J. & Lutsiv, T. Natural products in precision oncology: Plant-based small molecule inhibitors of protein kinases for cancer chemoprevention. *Nutrients* **15** (5), 1192 (2023).
10. Khan, M. et al. Inhibitory effect of natural compounds on dihydropteroate synthase of Mycobacterium Leprae: molecular dynamic study. *J. Biomol. Struct. Dynamics*. **41** (23), 13857–13872 (2023).
11. Johnson, M. et al. NCBI BLAST: a better web interface. *Nucleic Acids Res.* **36** (suppl_2), W5–9 (2008).
12. Wiederstein, M. & Sippl, M. J. ProSA-web: interactive web service for the recognition of errors in three-dimensional structures of proteins. *Nucleic Acids Res.* **35** (suppl_2), W407–W410 (2007).
13. Colovos, C. & Yeates, T. O. Verification of protein structures: patterns of nonbonded atomic interactions. *Protein Sci.* **2** (9), 1511–1519 (1993).
14. Eisenberg, D., Lüthy, R. & Bowie, J. U. [20] VERIFY3D: Assessment of Protein Models With three-dimensional Profiles. InMethods in Enzymology 1997 Jan 1 (Vol. 277, pp. 396–404). Academic.
15. Laskowski, R. A., MacArthur, M. W., Moss, D. S. & Thornton, J. M. PROCHECK: a program to check the stereochemical quality of protein structures. *J. Appl. Crystallogr.* **26** (2), 283–291 (1993).
16. Yun, M. K. et al. Catalysis and Sulfa drug resistance in dihydropteroate synthase. *Science* **335** (6072), 1110–1114 (2012).
17. Abdallah, E. M. Antibacterial activity of Hibiscus sabdariffa L. calyces against hospital isolates of multidrug resistant acinetobacterbaumannii. *J. Acute Disease*. **5** (6), 512–516 (2016).
18. Chou, S. T. et al. Exploring the effect and mechanism of Hibiscus sabdariffa on urinary tract infection and experimental renal inflammation. *J. Ethnopharmacol.* **194**, 617–625 (2016).
19. Knezevic, P. et al. Antimicrobial activity of Eucalyptus camaldulensis essential oils and their interactions with conventional antimicrobial agents against multi-drug resistant acinetobacterbaumannii. *J. Ethnopharmacol.* **178**, 125–136 (2016).
20. Dallakyan, S. & Olson, A. J. Small-molecule library screening by docking with PyRx. Chemical biology: methods and protocols. :243 – 50. (2015).
21. López-López, E., Naveja, J. J., Medina-Franco, J. L. & DataWarrior An evaluation of the open-source drug discovery tool. *Expert Opin. Drug Discov.* **14** (4), 335–341 (2019).
22. Chen, X. et al. Analysis of the physicochemical properties of acaricides based on Lipinski's rule of five. *J. Comput. Biol.* **27** (9), 1397–1406 (2020).
23. Daina, A., Michielin, O. & Zoete, V. SwissADME: a free web tool to evaluate pharmacokinetics, drug-likeness and medicinal chemistry friendliness of small molecules. *Sci. Rep.* **7** (1), 42717 (2017).
24. Morris, G. M. et al. AutoDock4 and AutoDockTools4: automated Docking with selective receptor flexibility. *J. Comput. Chem.* **30** (16), 2785–2791 (2009).
25. Spoel, D. V. et al. GROMACS: fast, flexible, and free. *J. Comput. Chem.* **26** (16), 1701–1718 (2005).
26. Zoete, V., Cuendet, M. A., Grosdidier, A. & Michielin, O. SwissParam: a fast force field generation tool for small organic molecules. *J. Comput. Chem.* **32** (11), 2359–2368 (2011).
27. Field, C. G. A force field for drug-like molecules compatible with the CHARMM all-atom additive biological force fields. *J. Comput. Chem.* **31**, 671–690 (2010).
28. Dick, T. J. & Madura, J. D. A review of the TIP4p, TIP4p-ew, TIP5p, and TIP5p-e water models. *Annual Rep. Comput. Chem.* **1**, 59–74 (2005).
29. McGibbon, R. T. et al. MDTraj: a modern open library for the analysis of molecular dynamics trajectories. *Biophys. J.* **109** (8), 1528–1532 (2015).
30. Kumari, R., Kumar, R., Open Source Drug Discovery Consortium & Lynn, A. g_mmpbsa A GROMACS tool for high-throughput MM-PBSA calculations. *J. Chem. Inf. Model.* **54** (7), 1951–1962 (2014).
31. Kumari, R. & Dalal, V. Identification of potential inhibitors for LLM of Staphylococcus aureus: structure-based pharmacophoremodeling, molecular dynamics, and binding free energy studies. *J. Biomol. Struct. Dynamics*. **40** (20), 9833–9847 (2022).
32. Dalal, V. & Kumari, R. Screening and identification of natural product-like compounds as potential antibacterial agents targeting FemC of staphylococcus aureus: an in-silico approach. *ChemistrySelect* **7** (42), e202201728 (2022).

Acknowledgements
Mr Saurabh Kumar Bhati wants to thank CSIR, New Delhi, India for fellowship. The authors also extend thanks to Sharda University for support. The authors also extend their appreciation to Taif University, Saudi Arabia for supporting this work through project number (TU-DSPP-2024-140).

Author contributions
Saurabh Kumar Bhati - Data curation, Formal analysis, Methodology, Software, Visualization, Writing - Original draft, Writing - review and editing. Rashmi Prabha Singh - Formal analysis, Supervision, Validation. Monika Jain - Formal analysis, Methodology, Software, Validation, Writing - review and editing. Jayaraman Muthukumaran - Investigation, Supervision, Validation, Software. Amit Kumar Singh - Conceptualization, Investigation, Supervision, Validation, Software. Farah Anjum - Investigation and Validation. Anas Shamsi - Investigation and Validation. Md Imtaiyaz Hassan – Analysis and Validation.

Declaration

Competing interests
The authors declare no competing interests.

Running title
Computational approach to find natural inhibitors for *Acinetobacter baumannii*.

Saurabh Kumar Bhati
Data curation, Formal analysis, Methodology, Software, Visualization, Writing- Original draft, Writing- review and editing.

Rashmi Prabha Singh
Formal analysis, Supervision, Validation.

Monika Jain
Formal analysis, Methodology, Software, Validation, Writing- review and editing.

Jayaraman muthukumaran
Investigation, Supervision, Validation, Software.

Amit Kumar Singh
Conceptualization, Investigation, Supervision, Validation, Software.

Farah anjum
Investigation and Validation.

Anas Shamsi
Investigation and Validation.

Md Imtaiyaz Hassan
Analysis and Validation.

Declaration of competing interest
The authors declare that they have no known competing financial interests or personal relationships that could have appeared to influence the work reported in this paper.

Additional information
Supplementary Information The online version contains supplementary material available at https://doi.org/10.1038/s41598-025-90946-9.

Correspondence and requests for materials should be addressed to A.S. or A.K.S.